ASSEMBLING LIGHT CURVES OF ZTF SUPERLUMINOUS SUPERNOVAE

Deepnika Jain[1]

—

Mentor: S.R. Kulkarni[2]

—

Co-Mentors: Lin Yan[2] And Christoffer Fremling[2]

—

[1] *National Institute of Technology Karnataka, India*
[2] *California Institute of Technology*

ABSTRACT

A star that collapses under its own gravitational force, results in a core-collapse supernova (CC-SN). Superluminous supernovae (SLSNe) are CC SNe which can be about a 100 times more luminous than an average CC SN. The extra luminosity in Type-I SLSNe is generally explained by the formation of magnetar; supported by high rise time and hence high total energy; where the massive magnetic energy is transferred to surrounding supernova ejecta. Interestingly, the late time spectra of SLSNe-I closely resembles that of Type Ic CC SNe. The luminosity of Type Ic SNe can be explained by radioactive decay of nickel formed when the core of the progenitor star collapses. It is possible that both of these classes always have some level of magnetar power and radioactive power at the same time, but the relative strength of the two varies. To gain more insight into the powering mechanism and relation between these two types, high quality lightcurves needed for model fitting are produced by reprocessing ZTF pipeline data. This method performs forced point spread function (PSF) photometry. SN fluxes at quiescent phases are recomputed and errors rescaled to apply any existing offsets to the pipeline data. Non-detections over carefully selected multi-epoch are coadded using inverse flux model to achieve better depths. This coherent lightcurve database can be directly fed into modeling softwares to derive physical parameters.

1. INTRODUCTION

Core-collapse supernovae (CC SNe) are a class of supernovae caused by gravitational collapse of their progenitor stars. During the last decade, it has been found that some CC SNe seem to out shine all others. These superluminous supernovae (SLSNe) can be up to a hundred times brighter than a normal CC SN.

SLSNe of Type II; SLSNe-II can be explained in a relatively straight-forward way by the presence of an exceptionally thick circumstellar medium surrounding the progenitor star (these show strong hydrogen signatures in their spectra). SLSNe-I do not show any sign of circumstellar material. To explain the extra luminosity in these events, one popular model is that a magnetar is formed when the core of the progenitor star collapses, and that energy from the strong magnetic fields surrounding the magnetar is transferred into the supernova ejecta, driving the extra luminosity. SLSN-I light curves evolve over much longer time scale (2-5 times longer). The long rise time and high luminosity imply much more total energy. This is the driver for magnetar model.

One interesting observational fact about SLSN-I is that as time passes and the luminosity declines, their spectra start to closely resemble those of normal CC SNe of Type Ic. Type Ic SNe belong to a class called Stripped-Envelope (SE) CC SNe, and they originate from very massive stars that lose their outer envelopes due to strong stellar winds, or from stars in binary systems where one star is stripped of its outer envelope due to tidal forces. It has been shown that the luminosity of the majority of "normal Type Ic SNe can be explained by radioactive decay of nickel formed when the core of the progenitor star collapses. However, there is a large range in the luminosity observed for Type Ic SNe, and some are very close to being just as bright as SLSN-I. Our objective is studying the optical lightcurves of SE SNe and SLSNe, and in particular focus on the transi-

tion from normal Type Ic SNe to SLSNe-I. The main questions we want to answer are:

- What is the range of possible light-curves for SLSNe-I?
- Could there be normal Type Ic SNe that are in fact more easily explained if they are powered by a magnetar instead of radioactive decay? Is it also possible that both of these classes always have some level of magnetar power and radioactive power at the same time, but the relative strength of the two varies.

In order to investigate the powering mechanism of these SNe and to meet the above goal, we need high quality lightcurves of all SLSNe and SE SNe thus far discovered by ZTF. We produce a coherent database of light curves which can be directly fed into modeling softwares to derive physical parameters.

2. UNDERSTANDING ZTF DATABASE

The ZTF camera is mounted on the 48-inch Samuel Oschin Telescope (P48) at Palomar Observatory (Dekany et al. 2016). ZTF divides its observing time between public surveys (40%), partnership surveys (40%), and Caltech surveys (20%). Each night's schedule is arranged by the survey scheduler (Bellm et al. 2019a) to optimize volumetric survey speed (Bellm 2016). At a limiting magnitude of r $\sim$ 20.5, three custom filters (gZTF, rZTF, and iZTF) are designed to maximize throughput by avoiding major skylines at Palomar. The current ZTF alert distribution system (Patterson et al. 2019) generates a source packet once a transient is detected. By definition, a "detection" means that the observed flux is 5 times larger than the flux uncertainty (see Masci et al. 2019, Section 6). While the individual ZTF alert packets contain a short baseline of historical detections, a complete historical record of variability is compiled via the GROWTH Marshal (Kasliwal et al. 2019) following the association of all alerts generated at the same position. The GROWTH Marshal is further used to aggregate and visualize follow-up spectra and transient classifications.

3. DATA ANALYSIS

3.1. *Initial Data*

The ZTF Science Data System (ZSDS) constructs reference images for each field and filter by taking the stack-average of 15 - 40 historical images. Observations for each target may be covered by multiple fields. To ensure that the reference image does not contain contamination from SN flux, we need to treat each field (with specific CCD-quadrant therein) for a given filter separately. Hereafter we use "fcqf" ID, defined by

$$\text{(fcqf ID)} = \text{(field ID)} \times 10000 + \text{(CCD ID)} \times 100 + \text{(quadrant ID)} \times 10 + \text{(filter ID)}$$

as an identifier of the reference images. Then, we group observations by fcqf ID. We perform forced-PSF photometry on these sources, as described in further sections.

3.2. *Forced PSF-fit Photometry*

3.2.1. *Coordinate Determination*

As the first step of forced photometry, we need to determine the position of the transient more accurately based on all observations where the SN is detected. To this end, for each target, we query the coordinates in all of its alert packets using Kowalski, a ZTF database and take the median of R.A. and Decl. as the re-centered coordinate.

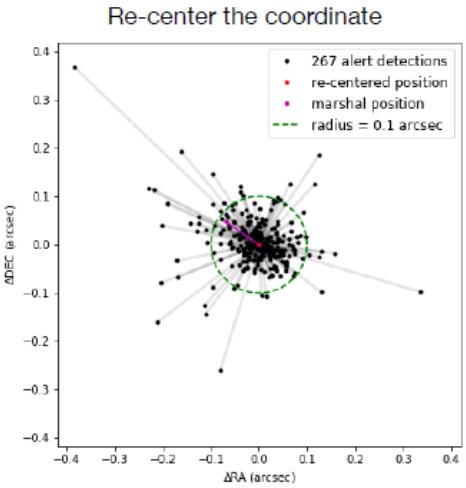

Figure 1. Calculating the re-centered coordinate for refined astrometry.

3.2.2. *The PSF Fitting Method*

We adopted a linear model y = mx for the PSF photometry, where m is the PSF-fit flux in the unit of DN. By definition, m = 0 when the source isn't detected. The statistical pixel uncertainty for y_i is

$$\sigma_i^2 = \frac{y_i}{g_i} + \sigma_{bkg}^2 \quad (1)$$

where g_i is the gain-factor in unit of DN/eletron. Although our task is simply getting a straight line to a set of data, there is no consensus on how to derive the best

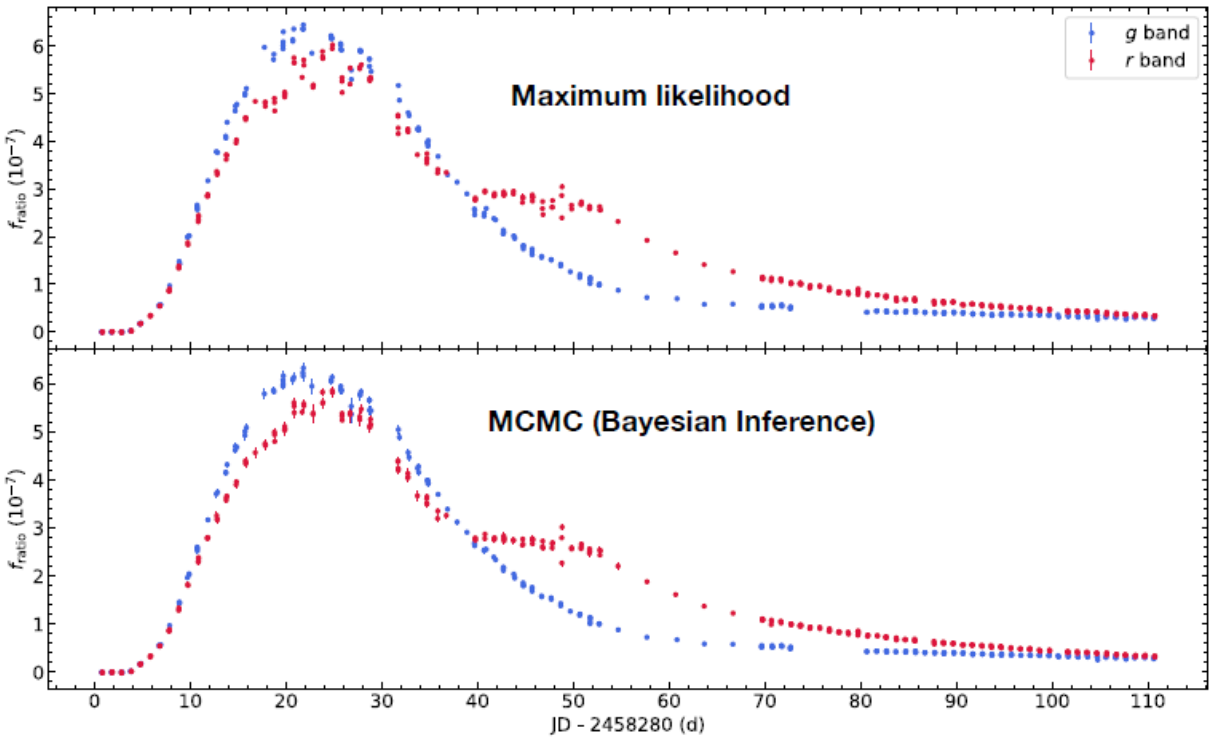

Figure 2. Comparison Between normal PSF-fit Photometry and Forced PSF-fit Photometry. Smoother fit at the peak is observed using emcee package.

measurement of m. Maximum likelihood estimate is optimal for the background-dominated-noise limit (Zackay et al. 2016). In this paper, we adopt the Markov Chain Monte Carlo (MCMC) based Bayesian statistics. In particular, we utilized emcee, which is an affine invariant MCMC ensemble sampler that uses multiple walkers to sample the posterior probability distribution.

We obtain the posterior probability distributions for m and σ_0 (a constant systematic factor representing the underestimation in uncertainties of y_i) as the output from the MCMC fitting, and marginalize over σ_0 to estimate the slope, m. Throughout this paper, we take the median value of the distribution as the measured flux, *fmcmc*, in unit of DN, whereas the uncertainty of this value, σ_{fmcmc}, is estimated by half of the difference between the 84th and 16th percentiles of the posterior of m.

3.3. *Quality Filtering*

A small fraction of the ZTF data was acquired through intermittent cloud cover and/or was contaminated by the moon. This would have impacted the photometric calibration. Therefore, several cuts were applied to ensure the quality of our photometric measurements.

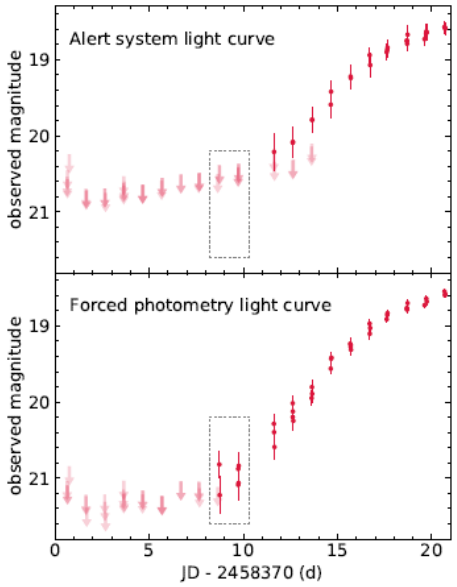

Figure 3. Upper panel: the r-band light curve of a sample generated by the alert distribution system. Bottom panel: Forced-PSF photometry light curve of the same object. The dotted box highlights additional early-time r-band detections recovered by forced photometry.

Forced Photometry from IPAC service was requested to get this information.

- We removed data points with non-zero values of infobits. Infobits is a 16-bit integer that encodes the status of processing and instrumental calibration steps for the science image; specific operations that fail to meet predefined quality criteria are assigned to individual bits [0..15]. These bits can be used to reject science images that failed specific calibration steps.
- We removed data points with scisigpix>25. Scisigpix is a robust estimate of spatial noise-sigma per pixel in input science image.
- We removed data points with seeing>6, where seeing captures FWHM of the point source.
- We removed the observation if there was any pixel in the central 7×7 cutout with y_i<-500. Typically, pixels with negative values of several hundreds are caused by saturation in the reference image, and thus should be removed in the fitting.

The Forced Photometry package does not have access to Partnership data (MSIP data; program ID = 1) recorded in 2019. That data was collected from Marshal.

3.4. *Query Kowalski*

This step is performed if we need baseline correction. Baseline correction, which is the next step, requires flux and field ID. Different combinations of field ID and filter have different reference images and therefore different offsets. The data from Marshal does not contain these fields and hence we need to query Kowalski database. We pull out jd, filter, programID, field, magzpsci, magzpsciunc. The following formulae can be used to get useful data:

$$f_0 = 10^{0.4zp} \tag{2}$$

$$f_0 = f_0 \times \sigma_{zp} ln(10)/2.5 \tag{3}$$

$$f_{mcmc} = f_{ratio} \times f_0 \tag{4}$$

3.5. *Baseline Correction*

For a given field and filter in the output flux, it is recommended to examine a plot of flux, *fmcmc* [DN] versus time [JD] to determine if there is any residual offset in the "baseline". The baseline here refers to the level defined by either historical or future epochs, where the transient signal relative to the reference image is stationary in time, relative to the background noise. For example, if the reference image used to generate the difference images was contaminated by the transients flux, the baseline will be <0. The reference image may also have been affected by some other systematic in its generation or calibration, and therefore the baseline could be >0.

Since the reference images for different fcqf ID were created by different observations, the baseline level should be determined separately for every possible combination of field and filter. For each combination of ffID (a variable made using field and filter), we determine the baseline region by eye. We visually inspect the light curves to find a quiescent phase which can be considered as the baseline. We remove any outliers with respect to a weighted flux average (>3 x Standard Deviation). It was made sure that no supernova flux was included in the baseline.

We then calculate the reduced chi square statistics (${\chi_\nu}^2$) for each possible combination of filter ID and field ID; where, N_{base} is the number of observations in each ffID in the baseline region; $\nu = N_{base}$ - 1 is the degree of freedom and C is the offset level calculated as the weighted mean of all fmcmc measurements in the baseline.

$$\chi^2_\nu = \frac{1}{\nu} \sum_{i=1}^{N_{base}} \frac{(C - f_{mcmc,i})^2}{\sigma^2_{fmcmc,i}} \tag{5}$$

Although we may expect C $\sim$ 0, a non-zero historical baseline level can occur if:

- The reference image is contaminated by residual flux from the actual transient being measured, i.e., the input images used to construct the reference inadvertently included epochs containing significant transient flux.
- Systematic residuals from persistently inaccurate gain-matching between the science and reference images.

Large values of offset and chi square should be considered as red flags and the image should be subjected to visual inspection. We mitigate this by subtracting the baseline C from the measured f_{mcmc}, and if ${\chi_\nu}^2$ >1, we multiply the raw σ_{fmcmc} by $\sqrt{{\chi_\nu}^2}$ for rescaling the error.

3.6. *Coadding*

To make your lightcurve measurements more statistically significant and with tighter upper-limits, we combine the flux measurements within carefully selected

Figure 4. Lightcurve after quality filtering

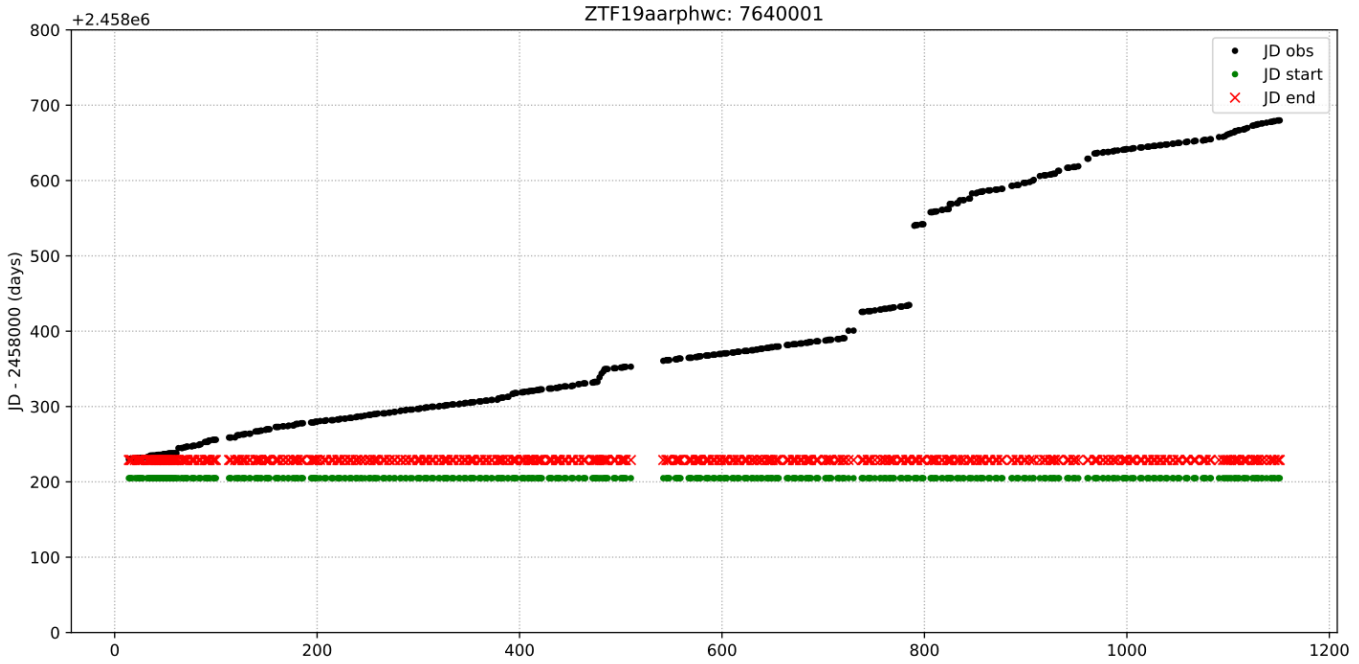

Figure 5. Checking whether the reference image contains supernova signal. We can compare the jdrefstart and jdrefend with the approximate jd of explosion.

time-windows. This procedure assumes that the single-epoch fluxes have been corrected for any non-zero baseline and uncertainties have been validated and rescaled if necessary. We use a method in which we assume

```
Compute Offset?
y
Please enter startjd-2458000:
600
Please enter endjd-2458000:
700
```

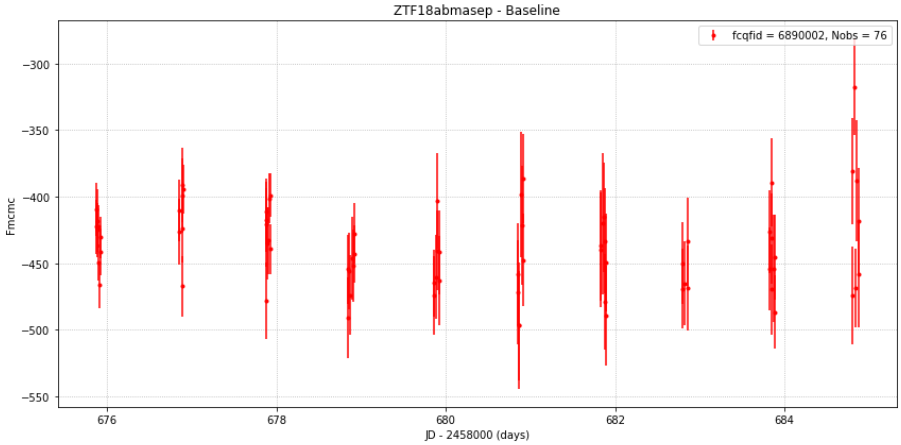


```
Remove Outliers?
y
Standard Deviation:  28.150454714947177 about Fmcmc =  -435.5089408393057
```

Figure 6. Baseline Correction in process.

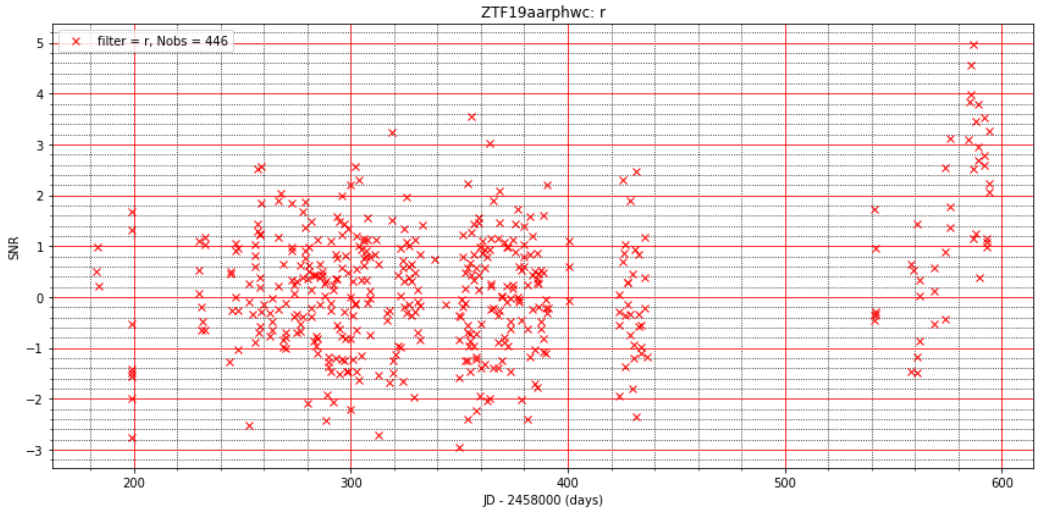


```
Coadd?
y
Please enter startjd-2458000:
590
Please enter endjd-2458000:
600
Found a real detection.

Fratio =  3.5777311804325548e-09

Fratio_unc =  5.186995202910135e-10

SNR =  6.897502389100511
```

Figure 7. Coadd in process

the underlying source signal is stationary within a time-window and collapse the single-epoch fluxes therein using an inverse-variance weighted average.

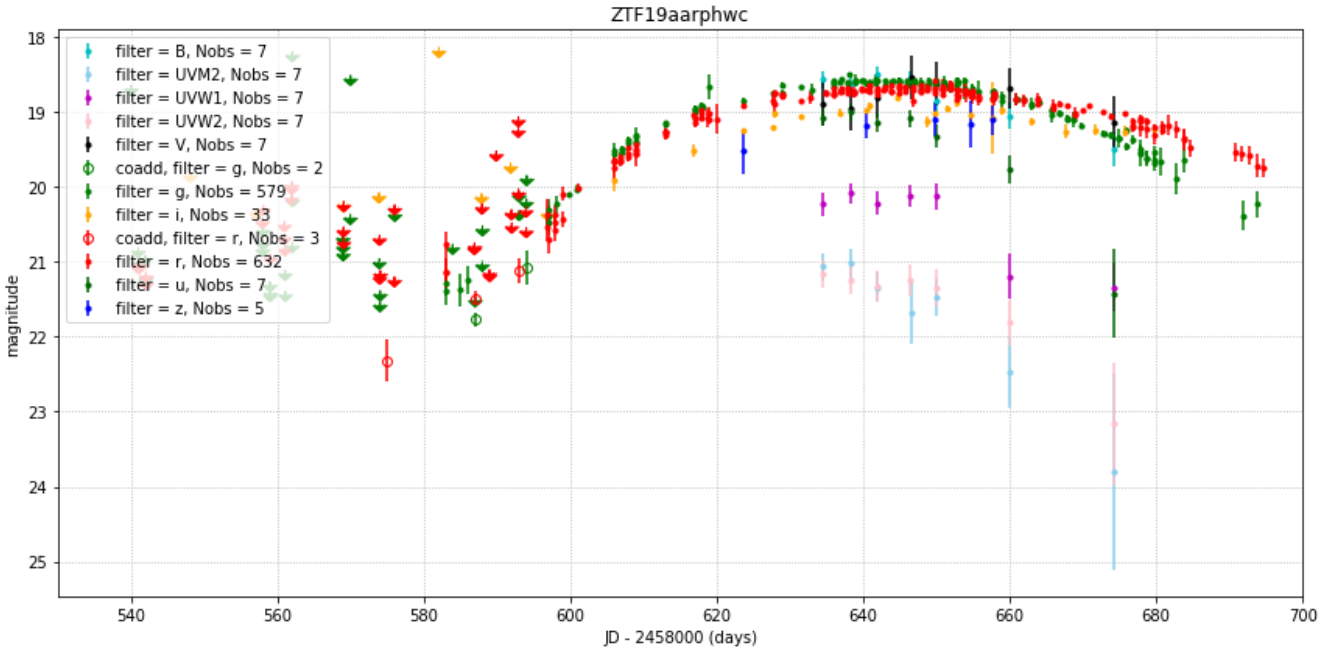

Figure 8. Final Lightcurve

$$Flux = \frac{\Sigma[w_i \cdot f_{mcmci}]}{\Sigma w_i} \quad (6)$$

where

$$w_i = \frac{1}{\sigma^2_{f_{mcmc_i}}} (7)$$

$$Fluxunc = [\Sigma w_i]^{-1/2} \quad (8)$$

and JD is the median of observed JDs.

The window for coadd should be narrow so as to avoid misplacing of the coadd data point with respect to JD. The Signal to Noise Ratio (SNR) threshold for coadd is 5 and the actual SNR for declaring a coadd to be valid is 3. We finally combine the data from other telescopes and display in magnitude space (Figure 8) for better understanding. This gives us a coherent database which can be directly fed into the modeling softwares.

4. ACKNOWLEDGMENTS

An opportunity to conduct research at Caltech is a huge confluence of motivation and opportunity. I am grateful and I want to thank Dr. Shrinivas R. Kulkarni for giving me this opportunity. I am also grateful to my co-mentors Dr. Lin Yan and Dr. Christoffer Fremling for their remarkable support and helping me on a daily basis. I also received great help from PhD student Yao Yuhan at Caltech. She is the author of the Forced Photometry Package and I look up to her as an inspiration. The Student-Faculty Programs office, thank you for your great hospitality; especially Asst. Director Carol Casey. I hope that this can be a starting point of something incredible for me. This research is my first experience and I hope to continue learning more about astronomy and astrophysics.

REFERENCES

[1]Generating Lightcurves from Forced PSF-fit Photometry on ZTF Difference Images, Frank Masci and Russ Laher

[2]Type Ia Supernovae Observed by ZTF in 2018. I: Light Curves and Sample Properties, Yuhan Yao et. al.